



## MOLECULAR DOCKING BASED ANTIDIABETIC SCREENING OF *CURCUMA CAESIA* ROXB.

Jyoti Rath<sup>1\*</sup>, Samriti Faujdar<sup>2</sup>, Anju Dhiman<sup>3</sup>, Rasana Yadav<sup>4</sup>, Pradeep Kumar<sup>5</sup>

### ABSTRACT

High blood glucose levels are a long-term metabolic condition known as diabetes mellitus (DM). In most cases, the hyperglycemic syndrome causes vascular damage and chronic nerve loss. Type 2 diabetes is the most prevalent and has spread over the entire planet. Controlling levels of blood glucose has remained a contentious problem for sufferer despite the development of numerous treatment strategies to control type 2 DM. The majority of prescription medications can have a variety of adverse effects, including gastrointestinal issues. So there is a significant demand for the creation of novel, effective anti-diabetic medicine with fewer side issues. In this study, different computational tools were used, including molecular docking and ADME tests of components of *Curcuma caesia* against alpha-amylase, alpha-glucosidase, and dipeptidase receptor. According to molecular docking studies, the alpha-amylase receptor binding pocket of the targeted drug (PDB ID: 4GQR) for coniferol, bisdemethoxycurcumin, desmethoxycurcumin, and curcumin all shown good docking scores. The selected (PDB ID: 6C9X) for alpha-glucosidase receptor compound Xanthinin, Dibutyl phthalate, Desmethoxycurcumin, and Aconerol showed good docking scores within binding pockets. The molecules Ivalin, Dibutyl phthalate, Terpinen-4-ol, and Argabin showed a superior docking scores within the binding pocket of the chosen (PDB ID: 1ITU) for dipeptidase receptor, and these substances can be employed as lead molecules for rational drug advancement. According to ADME research, the substances Aconerol, Argabin, Bisdemethoxycurcumin, Coniferol, Curcumin, Desmethoxycurcumin, Dibutylphthalate, Ivalin, Terpinen-4-ol, and Xanthinin fall under the parameters of the five rule of Lipinski. The research revealed that the constituents (Aconerol, Argabin, Bisdemethoxycurcumin, Coniferol, Curcumin, Desmethoxycurcumin, Dibutyl phthalate, Ivalin, Terpinen-4-ol, and Xanthinin) respond to Lipinski's rule, making them suitable lead molecules for more research.

**Keywords:** ADME, ant-diabetic activity, *Curcuma caesia*, curcumin, molecular docking.

<sup>1\*,2</sup>Department of Pharmacy, Banasthali Vidyapith, Rajasthan- 304022

<sup>3</sup>Department of Pharmaceutical Sciences, Maharshi Dayanand University, Rohtak – 124001

<sup>4</sup>Faculty of Pharmacy, The Maharaja Sayajirao University of Baroda, Gujarat- 390002

<sup>5</sup>Department of Pharmaceutical Sciences and Natural Products, Central University of Punjab, Ghudda, Bathinda, India- 151401

### \*Corresponding Author

Jyoti Rath, Department of Pharmacy, Banasthali Vidyapith, Rajasthan- 304022, Email: jyotirathee.angle@gmail.com

**DOI:** - 10.31838/ecb/2023.12.si5.0112

## INTRODUCTION

Diabetes mellitus (DM) is a chronic metabolic condition characterised by persistent increases in blood sugar levels, high serum triglycerides, polyuria, polyphagia, and polydipsia<sup>[1, 2]</sup>. Elevated blood glucose levels, which are a symptom of type 2 diabetes mellitus (T2DM), are a dangerous, long-term metabolic illness brought by insufficient insulin production or insulin resistance<sup>[3]</sup>. 463 million persons (20-79 years) in India were estimated with DM, and by 2045, that figure is expected to rise to 700 million<sup>[4]</sup> according to estimates from the International Diabetes Federation (IDF). According to data from 2019, there are 87.9 million people with DM living in the South East Asia Region, the disease's epicentre, of which 34.3 percent reside in cities and 49.4 percent in rural regions<sup>[5]</sup>. In middle-income South Asian nations, the vast majority of people (99.2%) have DM. A frequency of 8.7% in the adult population has been estimated for Sri Lanka, a developing country in South Asia (20 -79 age)<sup>[5]</sup>. Due of DM's long-duration effects, it has become one of the major global reasons of morbidity<sup>[6]</sup>. Based on the pathophysiology, diabetes can be categorised as insulin-dependent (type I), non-insulin-dependent (type II), or gestational.

The body's insulin receptors become resistant to the typical actions of insulin in Type 2 DM, which is more frequent than the other forms. In order to control the situation, the pancreas then generates more insulin in response to the increased blood glucose levels. However, excessive insulin synthesis causes cells to become exhausted<sup>[7, 8]</sup>.

As a result of chronic hyperglycemia, patients with DM may develop problems like retinopathy, cataracts, neuropathy, peripheral vascular insufficiencies, nephropathy, and damaged nerves<sup>[8-10]</sup>. For stopping the spread of the disease, various mechanisms and pathways are taken into account. They could include inhibiting intestinal alpha-glucosidase and amylase, insulin synthesis and secretion, protecting against oxidative stress, inhibiting the formation of advanced glycation end products, reduction of plasma glucose levels, alteration of hexokinase and glucose-6-phosphate enzyme activity, inhibiting postprandial hyperglycemia, stimulating GLUT-4, reduction of G6P activity<sup>[11, 8]</sup>.

The inhibition of important enzymes is one of the most widely used methods for controlling blood glucose levels<sup>[12]</sup>. Two carbohydrate digestion enzymes,  $\alpha$ -glucosidase and  $\alpha$ -amylase, can enhance postprandial hyperglycemia (PPHG). As

a result, their inhibition is crucial for managing PPHG in individuals with type 2 diabetes. While  $\alpha$ -amylase inhibition prevents the conversion of starch to glucose, inhibition of  $\alpha$ -glucosidase reduces the hydrolysis of disaccharides. In studies where these substances have been used, patients' blood glucose levels have been decreased<sup>[13, 14]</sup>. The most significant side effect of the FDA-approved type 2 DM medications, such as voglibose, sulphonylureas, acarbose, thiazolidine, and miglitol, is gastrointestinal distress, which requires further treatment. Investigation of various treatment options with fewer adverse effects is highly desired in the US<sup>[15-17]</sup>.

Important enzymes that impact the breakdown and absorption of starch and other carbohydrates in the diet are alpha-amylase and alpha-glucosidase<sup>[18]</sup>. Dextrin and oligosaccharides are produced from starch by the hydrolyzes of the alpha-D-1,4-glucosidic link by alpha-amylase, and glucose is produced from dextrin and oligosaccharides by alpha-glucosidase<sup>[19, 18]</sup>. The subsequent transfer of glucose to blood arteries raises postprandial blood glucose, resulting in obesity or diabetes<sup>[20, 21]</sup>. As a result, inhibiting alpha-amylase and alpha-glucosidase activity decreases starch digestibility and postpones starch breakdown and glucose absorption<sup>[22, 23]</sup>. Although acarbose and miglitol, two antihyperglycemic medications, now suppress the activities of alpha- amylase and glucosidase, certain negative side effects, such as diarrhoea, flatulence, and liver illness, can happen<sup>[24]</sup>. Because of this, polyphenols with a range of biological actions have been shown to be possible natural inhibitors of alpha-amylase and alpha-glucosidase activity<sup>[25]</sup>.

The perennial herb *Curcuma caesia* Roxb., often known as Kali haldi, is widespread in the Himalaya area, and central India. Leucoderma, asthma, tumours, piles, and other conditions have all been traditionally treated using rhizome paste. Alkaloids, steroids, phenolics, and tannins are some of the bioactive compounds that provide *C. caesia* for its therapeutic significance<sup>[26]</sup>. Several medicinal benefits of *C. caesia* have been scientifically documented, including antioxidant, larvicidal, pneumonia, antipyretic, antimicrobial, insecticidal, asthma, antihyperglycemic, haemorrhoids, menstrual problem, epilepsy, leucoderma, inflammation, etc.<sup>[27-28]</sup>. The rhizomes of *C. caesia* are said to contain a number of bioactive compounds, including flavonoids, curcumin, 1, 8-cineole, amino acids, alkaloids, ar-turmerone, curcuminoids, and phenolics<sup>[29-30]</sup>. These bioactive compounds were have been

documented for their pharmacological effects like anti-inflammatory, antimicrobial, antioxidant, anticoagulant, antimicrobial, hypoglycaemic<sup>[31]</sup>, smooth muscle relaxant<sup>[32]</sup>, anti-diabetic activity<sup>[33]</sup>, free-radical scavenging opposed to reactive oxygen, antitumour activity<sup>[34]</sup>, anti-mutagenic activity<sup>[35]</sup>, anti-mycobacterial activity<sup>[36]</sup> and antitoxicity against cyclophosphamide<sup>[37]</sup>.

The development of a new drug procedure is sped up by computer-aided drug designing (CADD), which extracts prospective lead molecules from large chemical libraries<sup>[38]</sup>. The pharmacokinetics of lead compounds are discovered and enhanced using CADD<sup>[39]</sup>.

The most effective orientation and conformation for a protein's ligand binding are the goals of a docking study, which also aids in finding the right molecule by screening through huge databases<sup>[40]</sup>. The time and budget of drug discovery have been reduced by the use of several computer tools in drug screening and design<sup>[41]</sup>. Accurate activity prediction and precise structural modelling are the key objectives of the docking investigation. The

molecular docking technique is used to investigate drug molecule orientation to the target site, drug-receptor interaction, and binding affinity<sup>[42]</sup>.

Pharmacokinetics, which is the study of how drugs are absorbed, distributed, metabolised, and excreted by humans, is defined by the Lipinski rule. Because of its low cost and great result, ADME modelling has drawn a significant research interest in the pharmaceutical industry<sup>[43]</sup>.


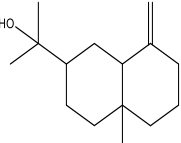
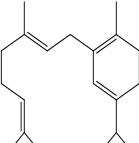
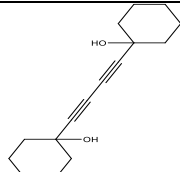
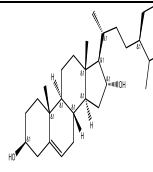
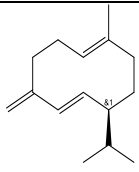
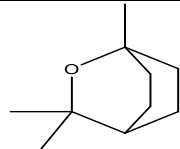
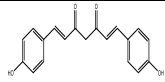
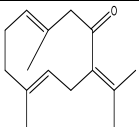
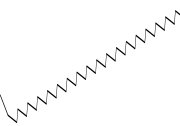
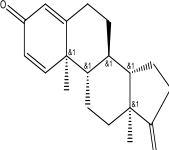
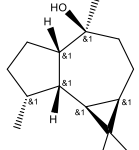
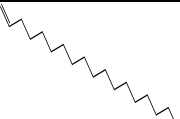
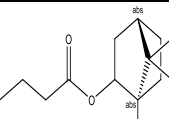
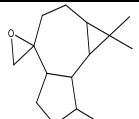
In response to the findings discussed above from the current investigation, we are reporting on the molecular docking and ADME analyses of bioactive constituents of *C. caesia* that were chosen from published work<sup>[44]</sup>.

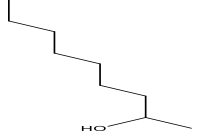
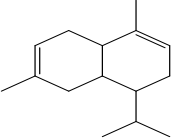
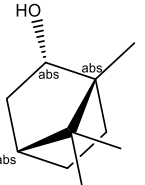
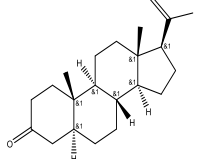
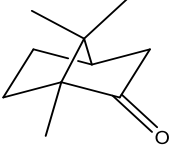
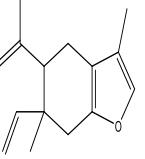
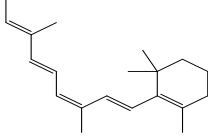
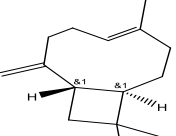
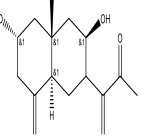
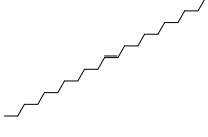
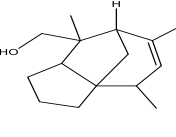
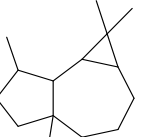
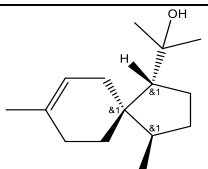
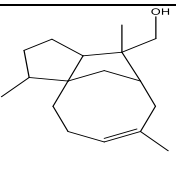
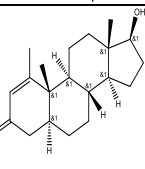
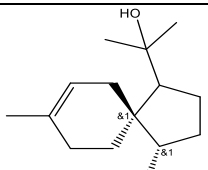
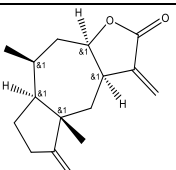

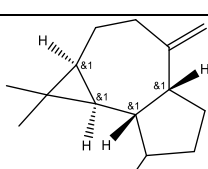
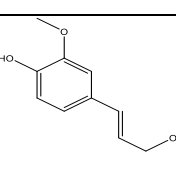
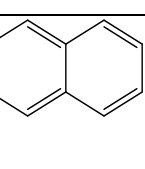
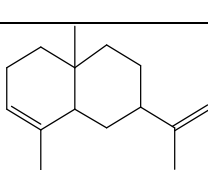
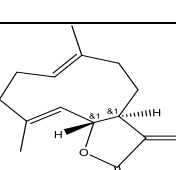
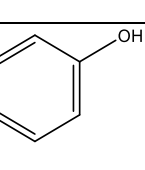
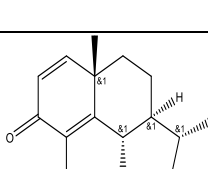
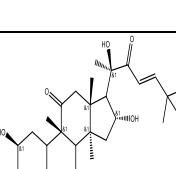
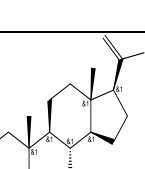
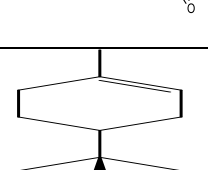
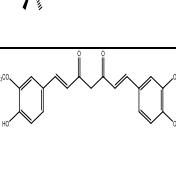
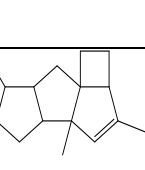
## MATERIAL AND METHODS

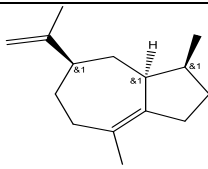
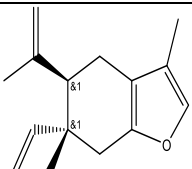
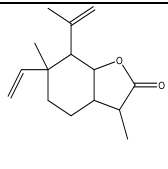
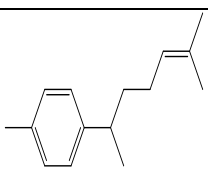
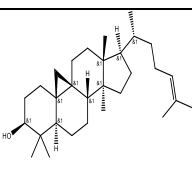
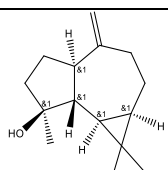
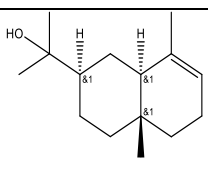
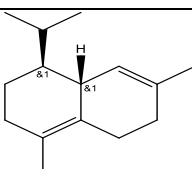
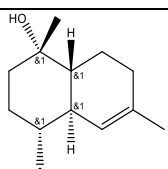
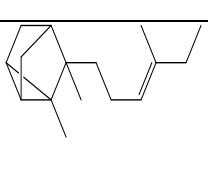
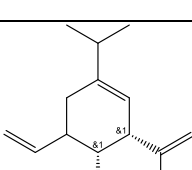
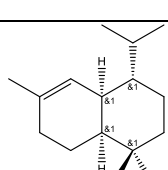
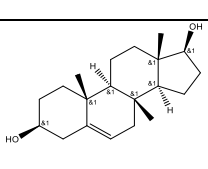
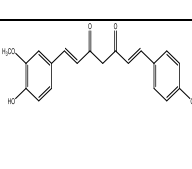
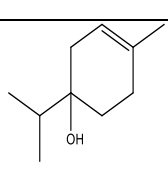
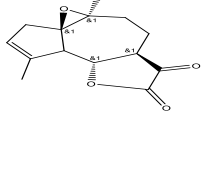
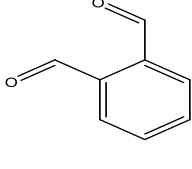
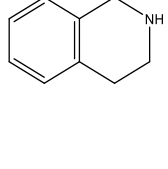
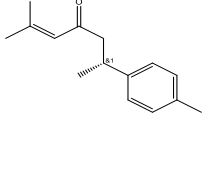
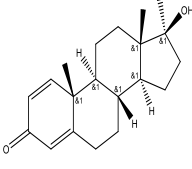
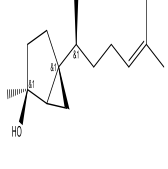
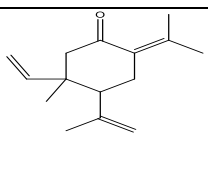
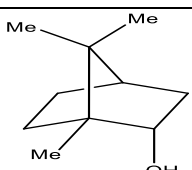
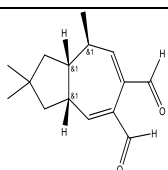
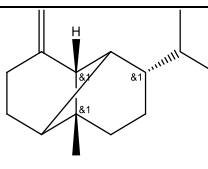
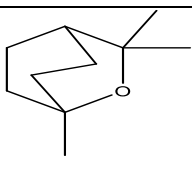
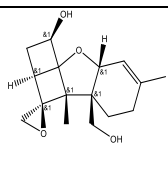
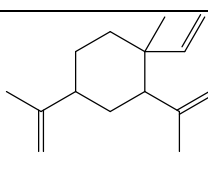
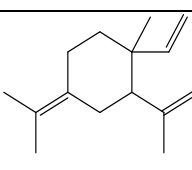
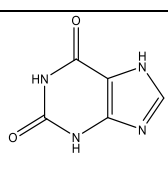
### Molecular docking study

The structures of 75 compounds of *C. caesia* were selected from published work<sup>[44]</sup>, sketched using ChemDraw 19.0, and are shown in Table 1. Schrodinger Suite 13.1 was used for the molecular docking

**Table 1:** Chemical Structure of compounds of *C. caesia* used in molecular docking

Compound Name	Chemical Structure	Compound Name	Chemical Structure	Compound Name	Chemical Structure
(+)-2-Bornanone		$\beta$ -Selinene		Geranyl- $\alpha$ -terpene	
1,1'-Butadiynylene dicyclohexanol		$\beta$ -Sitosterol		Germacrene D	
1,8-Cineole		Bisdemethoxycurcumin		Germacrone	
1-heptatriacotan ol		Boldione		Himabaccol	
1-Nonadecene		Bornyl ester		Isoaromadendrene epoxide	

<b>2-Nonanol</b>		<b>Cadinene</b>		<b>Isoborneol</b>	
<b>5 alpha-Dihydroproges terone</b>		<b>Camphor</b>		<b>Isofurano-germacrene</b>	
<b>9-cis-Retinal</b>		<b>Caryophyllene</b>		<b>Lvalin</b>	
<b>10-heneicosene</b>		<b>Cedr-8-en-13-ol</b>		<b>Ledene oxide-(1)</b>	
<b>17-chloro-alpha-acorenol</b>		<b>Cedren-13-ol</b>		<b>Methenolone</b>	
<b>Aconerol</b>		<b>Confertin</b>		<b>Methyl stearolate</b>	
<b>Alloaromadendrene</b>		<b>Coniferol</b>		<b>Naphthalene</b>	
<b>alpha-Selinene</b>		<b>Costunplide</b>		<b>Phenol</b>	
<b>alpha-Santonin</b>		<b>Cucurbitacin-B</b>		<b>Pregan-20-one</b>	
<b>alpha-Terpineol</b>		<b>Curcumin</b>		<b>Rotundene</b>	

<b><math>\alpha</math>-Bulnesene</b>		<b>Curzerene</b>		<b>Saussurea lactone</b>	
<b><math>\alpha</math>-Curcumene</b>		<b>Cycloartanol acetate</b>		<b>Spathulenol</b>	
<b><math>\alpha</math>-Eudesmol</b>		<b>Delta-cadinene</b>		<b><math>\tau</math>-Cadinol</b>	
<b><math>\alpha</math>-Santalol</b>		<b>Delta-elemene</b>		<b>T-Muurolol</b>	
<b>Androstenediol</b>		<b>Desmethoxycurcumin</b>		<b>Rerpinen-4-ol</b>	
<b>Arglabin</b>		<b>Dibutyl phthalate</b>		<b>Tetrahydroisoquinoline</b>	
<b>Ar-tumerone</b>		<b>Dimethandrostanolone</b>		<b>trans-Sesquisabinene hydrate</b>	
<b><math>\beta</math>-Elemenone</b>		<b>Endo-Borneol</b>		<b>Velleral</b>	
<b><math>\beta</math>-Copaene</b>		<b>Eucalyptol</b>		<b>Verrucarol</b>	
<b><math>\beta</math>-Elemene</b>		<b><math>\gamma</math>-Elemene</b>		<b>Xanthinin</b>	

### Protein preparation

Each atom must have charge and an atom type that identifies characteristics in order for docking algorithms to function. These characteristics are absent from the protein structure from the PDB that was downloaded. To incorporate these values in addition to the atomic coordinates, we must therefore generate the protein and ligand file. The Schrodinger suite's protein preparation wizard was carried out for the preparation of protein. The RCSB Protein Data Bank's high resolution downloads of the PDB IDs: 4GQR (for amylase), 6C9X (for glucosidase), and 1ITU (for dipeptidase) were processed in advance of further research. Atoms of hydrogen were added to ensure good docking electrostatic treatment. Bond order was created after the removal of water molecules<sup>[45]</sup>. To PH 7.4, the tautomeric and protonation states were produced. To prevent steric conflicts between the atoms, the optimization of atomic charges and minimization of energy protein were performed using the OPLS4 force field<sup>[46]</sup>.

### Ligand preparation

For the creation of 3D ligands that must interact with proteins in order to evaluate their anticancer potential, the mol2 file format is necessary. Using the maestro module, a number of heterocyclic molecules that were picked out of the literature were created. Their 3D mol data were transformed using the .maegz file with Ligprep supported software. Using the OPLS4 force field module, all ligands were minimised<sup>[47-48]</sup>. For generating and assessing ligand poses within the binding sites of receptors, docking includes a search algorithm and an energy scoring function<sup>[49]</sup>.

### Grid generation and molecular docking

The site map tool was used to construct the best grid for the preprocessed protein (4GQR, 6C9X, and 1ITU) around its most active site. The grid-generated receptor (the protein's active site) was combined with all of the prepared ligands after grid preparation, and docking was then performed under standard precision (SP) to produce the dock score values with the protein ligand conformational complexes that were most appropriate<sup>[48]</sup>.

### ADME study

Determining ADME characteristics is a crucial step because the majority of pharmaceutical substances fail in clinical trials. The likelihood and ADME characteristics of the most active components were ascertained using QikProp, GLIDE, and Schrodinger v 13.1. Schrodinger 13.1's LigPrep module was used to synthesise the ligand for the ADME study in Maestro format (.maez). Then, in order to retrieve the ADME parameters, we got to work by opening the QikPro dialogue box and inserting the ligand preparation file (.maez) for the synthesised derivatives<sup>[50]</sup>.

### RESULTS AND DISCUSSION

From a literature review, various series of curcumin derivatives were chosen (Table 1). Using the molecular docking programme Schrodinger v. 13.1, PDB IDs 4GQR, 6C9X, and 1ITU were used to calculate the antidiabetic compounds docking scores (Table 2) in relation to standard drug Acarbose and Glibenclamide.

**Table 2:** Docking rating of constituents of *C. caesia* using (PDB ID: 4GQR, 6C9X, and 1ITU)

Compound Name	Dockin g Score (PDB ID: 4GQR)	Dockin g Score (PDB ID: 6C9X)	Dockin g Score (PDB ID: 1ITU)	Compound Name	Dockin g Score (PDB ID: 4GQR)	Dockin g Score (PDB ID: 6C9X)	Dockin g Score (PDB ID: 1ITU)
(+)-2-Bornanone	-6.297	-5.707	-3.902	Cucurbitacin-B	-4.732	-3.343	-3.760
1,1'-Butadiynylene dicyclohexanol	-5.229	-6.185	-4.005	Curcumin	-7.093	-6.125	-4.533
1,8-Cineole	-5.564	-5.226	-3.969	Curzerene	-4.329	-4.736	-3.111
10-heneicosene	1.056	0.271	1.829	Cycloartanol acetate	-4.517	-4.216	-2.597
17-chloro-alpha- acorenol	-5.023	-3.662	-3.776	Delta-cadinene	-5.266	-3.668	-3.360
1-Nonadecene	2.858	1.782	2.842	Delta-elemene	-4.489	-4.372	-2.447
2-Nonanol	-2.853	-2.820	-1.986	Desmethoxycurcumi n	-7.119	-5.735	-4.882
5α- Dihydroprogesterone	-5.329	-3.300	-3.708	Dibutyl phthalate	-6.253	-7.185	-5.391
9-cis-Retinal	-5.318	-3.817	-2.682	Dimethanodrostanol one	-5.630	-4.016	-4.806
Acarbose	-7.370	-6.205	-4.697	Endo-Borneol	-5.423	-5.730	-3.828



<b>Aconerol</b>	-4.922	-6.778	-4.635	<b>Eucalyptol</b>	-5.564	-5.226	-3.969
<b>Alloaromadendrene</b>	-5.392	-3.361	-3.557	<b>-Elemene</b>	-4.600	-4.717	-2.863
<b><math>\alpha</math> – Selinene</b>	-5.184	-3.309	-3.141	<b>Geranyl-alpha-terpenene</b>	-3.984	-4.236	-2.512
<b><math>\alpha</math> - Santonin</b>	-5.412	-4.308	-3.963	<b>Germacrene D</b>	-5.313	-3.388	-3.967
<b><math>\alpha</math> - Terpineol</b>	-5.683	-5.579	-4.532	<b>Germacrone</b>	-5.395	-3.825	-3.512
<b><math>\alpha</math> -Bulnesene</b>	-5.676	-3.175	-4.109	<b>Himabaccol</b>	-6.243	-5.700	-3.786
<b><math>\alpha</math> -Curcumene</b>	-3.371	-4.119	-2.969	<b>Isoaromadendrene epoxide</b>	-5.516	-3.288	-3.908
<b><math>\alpha</math> -Eudesmol</b>	-5.809	-4.575	-4.562	<b>Isoborneol</b>	-5.716	-6.406	-4.114
<b><math>\alpha</math> -Santalol</b>	-4.050	-3.889	-2.251	<b>Isofurano-germacrene</b>	-4.329	-4.736	-3.111
<b>Arglabin</b>	-6.136	-3.937	-5.305	<b>Ivalin</b>	-4.808	-4.519	-5.087
<b>Ar-tumerone</b>	-4.674	-4.180	-3.618	<b>Ledene oxide-(1)</b>	-4.456	-4.221	-4.791
<b><math>\beta</math>- Elemenone</b>	-4.246	-4.949	-3.773	<b>Methenolone</b>	-6.808	-4.205	-4.295
<b><math>\beta</math> -Copaene</b>	-4.995	-3.207	-3.315	<b>Methyl stearolate</b>	0.553	-0.048	-0.131
<b><math>\beta</math> -Elemene</b>	-3.907	-2.636	-2.698	<b>Naphthalene</b>	-5.077	-5.405	-3.169
<b><math>\beta</math> -selinenol</b>	-4.869	-3.550	-4.750	<b>Phenol</b>	-5.695	-6.228	-4.118
<b><math>\beta</math> -Sitosterol</b>	-5.818	-4.383	-2.130	<b>Pregan-20-one</b>	-5.868	-3.208	-3.033
<b>Bisdemethoxycurcumin</b>	-7.293	-6.552	-4.237	<b>Rotundene</b>	-5.188	-3.907	-3.375
<b>Boldione</b>	-5.963	-4.020	-4.542	<b>Saussurea lactone</b>	-5.901	-4.173	-3.186
<b>Bornyl ester</b>	-3.580	-4.460	-2.774	<b>Spathulenol</b>	-5.591	-4.949	-4.708
<b>Cadinene</b>	-5.376	-3.339	-3.477	<b><math>\tau</math>- Cadinol</b>	-5.617	-3.867	-4.072
<b>Camphor</b>	-6.297	-5.707	-3.902	<b>T- Muurolol</b>	-5.588	-3.928	-4.371
<b>Caryophyllene</b>	-5.274	-5.743	-3.094	<b>Terpinen-4-ol</b>	-5.840	-5.700	-4.933
<b>Cedr-8-en-13-ol</b>	-5.804	-5.398	-3.765	<b>Tetrahydroisoquinoline</b>	-5.670	-6.600	-4.745
<b>Cedren-13-ol</b>	-5.939	-5.318	-3.102	<b>trans-Sesquisabinene hydrate</b>	-5.274	-4.363	-3.701
<b>Confertin</b>	-6.015	-4.063	-4.647	<b>Velleral</b>	-5.819	-3.971	-4.227
<b>Coniferol</b>	-7.367	-5.412	-4.711	<b>Verrucarol</b>	-4.206	-3.511	-3.399
<b>Costunolide</b>	-5.586	-3.633	-4.650	<b>Xanthinin</b>	-5.852	-8.167	-4.621

**Table 3:** Docking score of the most active constituents using PDB ID: 4GQR, and standard drug Acarbose, Glibenclamide)

Compounds Name	Score of Docking	Glide Emodel	Energy of Glide	Interconnecting Residues
<b>Coniferol</b>	-7.367	-47.747	-33.039	Asp197, Glh233, Trp59, Gln63, Glu60, Ala198, Arg195, Pro64
<b>Bisdemethoxycurcumin</b>	-7.293	-58.042	-40.426	Asp197, Asp300, Asp96, Hip305, Gln63, Ala198, Hie299, Glu60
<b>Desmethoxycurcumin</b>	-7.119	-63.998	-45.708	Glh233, Asp197, Gln63, Asp300, Cys103, Pro64, Thr163, Leu165
<b>Curcumin</b>	-7.093	-65.341	-46.407	Glh233, Asp197, Gln63, His201, Val98, Ser199, Asp300, Leu162
<b>Acarbose</b>	-6.808	-53.565	-37.845	Asp197, Asp300, Asp356, Trp59, Ile51, Hip305, Gly306
<b>Glibenclamide</b>	-4.525	-63.994	-46.77	Gln63, Hip305, Trp59, Thr163

Molecular docking was used to examine the means by which the components of *C. caesia* bind to the associated receptors. A molecular docking research was carried out using *C. caesia*'s compounds and a common drug at the active site of alpha-amylase (PDB ID: 4GQR) (acarbose, glibenclamide). The 2-D ligand interaction diagrammatic viewpoint suggests that the oxygen atom of the compound coniferol amide nucleus

formed interactions of hydrogen alongwith Trp59, Gln63, and Asp197 residues of amino acid. With oxygen atoms of the molecules Bisdemethoxycurcumin and Desmethoxycurcumin amide nucleus, amino acid residues Asp300, Asp197, and Gln63 formed hydrogen bonds.

Hydrogen bonds were formed between the oxygen atoms in the amide nucleus of the molecule

curcumin and the amino acid residues Asp197, Gln63, and water. Hydrogen bonds were formed between the oxygen atoms of the amide nucleus of the common drug acarbose and the amino acid residues Asp197, Gln63, Asp300, and Asp356. The figures for glide energy, docking scores, and glide emodel were displayed negatively.

The affinity of the ligand for interacting to the receptor increases as the score of docking decreases. Docking data for the top four substances (coniferol, bisdemethoxycurcumin,

desmethoxycurcumin, and curcumin), as well as the reference drug, are displayed in Table 3. The docked molecules coniferol, bisdemethoxycurcumin, desmethoxycurcumin, curcumin, and acarbose are shown in Figures 1, 2, 3, 4, 5 and 6 together with their respective binding surfaces and ligand interaction diagrams. The 2-D ligand interaction diagrammatic perspective reveals that these compounds bind with homologous residues of amino acid and have the same homology like regular acarbose

#### Binding surface & 2D interaction diagram of compounds of *C.caesia* using PDB ID: 4GQR

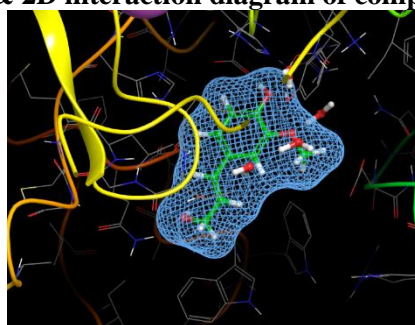


Figure1: Coniferol

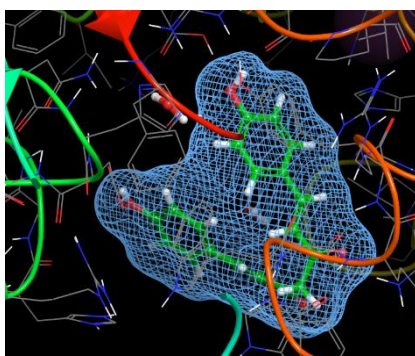
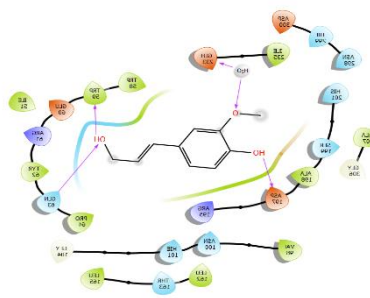


Figure 2: Bisdemethoxycurcumin

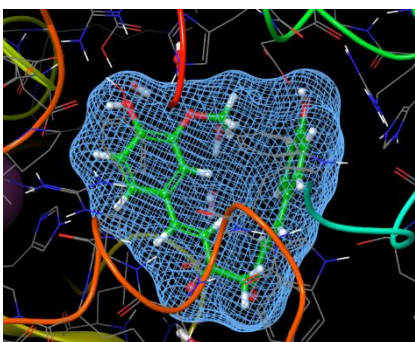
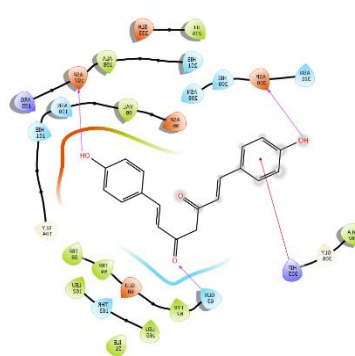
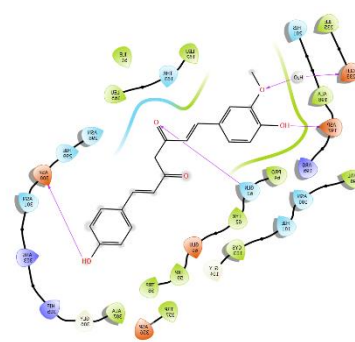
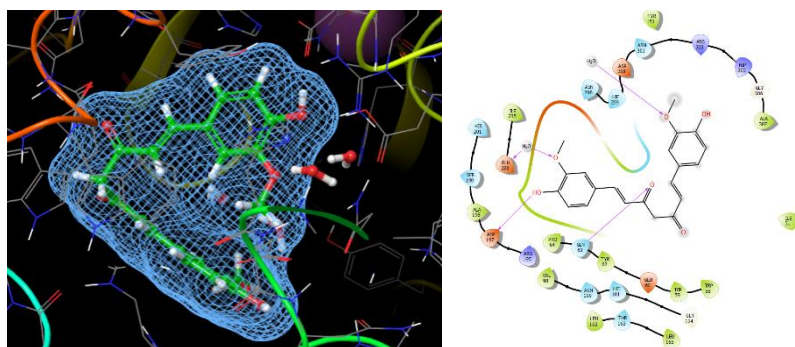
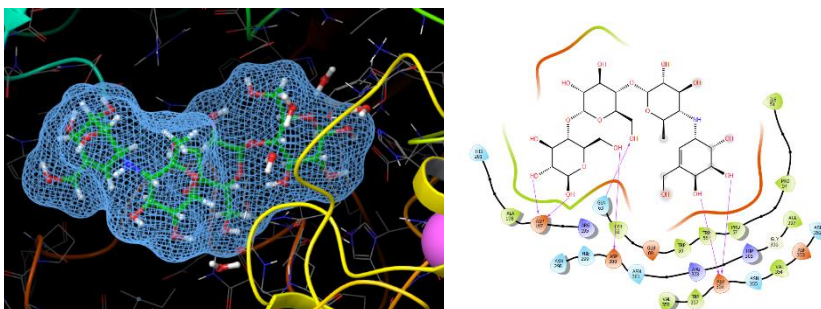
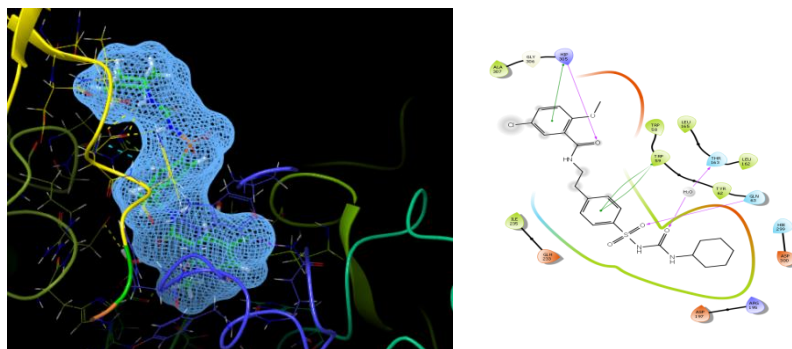


Figure 3: Desmethoxycurcumin





**Fig 4: Curcumin****Figure 5: Acarbose****Figure 6: Glibenclamide****Table 4:** Docking score of the most active components using PDB ID: 6C9X, and reference drug Acarbose, Glibenclamide

Compounds Name	Docking data	Glide Emodel	Glide Energy	Interrelating Residues
<b>Xanthinin</b>	-8.167	-50.464	-32.250	Asp420, Hie478, Asp197, Ala480, Met308, Trp271, Pro75, Phe453
<b>Dibutyl phthalate</b>	-7.185	-39.034	-27.924	Hie478, Ash26, Met308, Phe314, Arg476, Glu481, Tyr85, Trp417
<b>Aconerol</b>	-6.778	-38.604	-29.398	Hie478, Asp307, Met308, Glu481, Arg476, Gly419, Ash236, Ile234
<b>Desmethoxycurcumin</b>	-6.739	-68.918	-48.481	Trp169, Asp197, Arg404, Ala269, Hie478, Lys348, Met347, Trp271
<b>Acarbose</b>	-6.205	-76.306	-60.952	Hie478, Asp73, Glu481, Arg404, Asp197, Asp420, Asp449, Ser167
<b>Glibenclamide</b>	-4.727	-66.804	-50.824	Asp455, Arg404, Lys 422

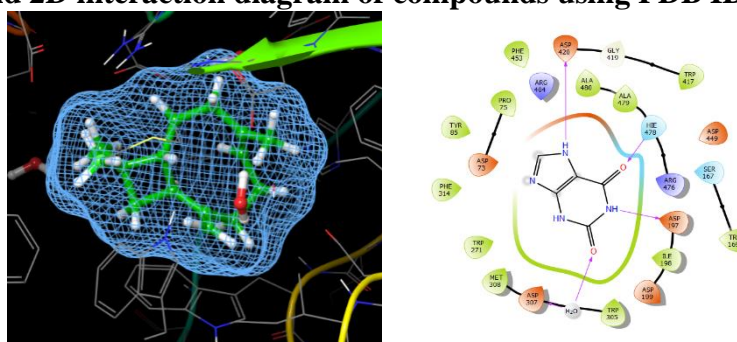
Molecular docking was used to examine the means by which the compounds of *C. caesia* bind to the associated receptors. We performed a *Eur. Chem. Bull.* **2023**, 12(Special Issue 5), 914 – 929

molecular docking analysis of *C. caesia* compounds and a conventional drug on the active site of alpha-glucosidase (PDB ID: 6C9X)

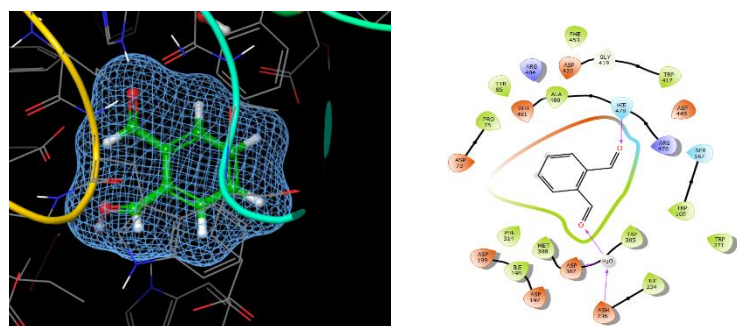
(acarbose). According to the 2-D ligand interaction, the oxygen atom of the molecules Xanthinin and Aconerol amide nucleus established hydrogen bonds with Hie478 residues of amino acid. Hydrogen bonds were produced between the amino acid residues of Hie478, Ash236, and water and the Dibutyl phthalate amide nucleus of the molecule. The oxygen atoms in the amide nucleus of desmethoxycurcumin and the residue of the amino acid Asp197 created hydrogen bonds. The amino acid residues Asp197, Glu481, Asp73, Arg404, Asp420, and Hie478 formed hydrogen bonds with the oxygen atoms of the amide nucleus of the common medication acarbose. The docking scores, glide energy, and glide emodel numbers

were displayed negatively. The ligand's affinity for binding to the receptor increases with decreasing docking score. The top four compounds (Xanthinin, Dibutyl phthalate, Desmethoxycurcumin, and Aconerol), as well as the reference drug, are shown in Table 4 along with their docking data. Figures 7, 8, 9, 10, 11 and 12 show the docked molecules Xanthinin, Dibutyl phthalate, Desmethoxycurcumin, Aconerol, and acarbose's respective binding surface and ligand interaction diagram. According to the 2-D ligand interaction diagrammatic perspective, these compounds have the same homology as regular norfloxacin by interacting with homologous amino acid residues.

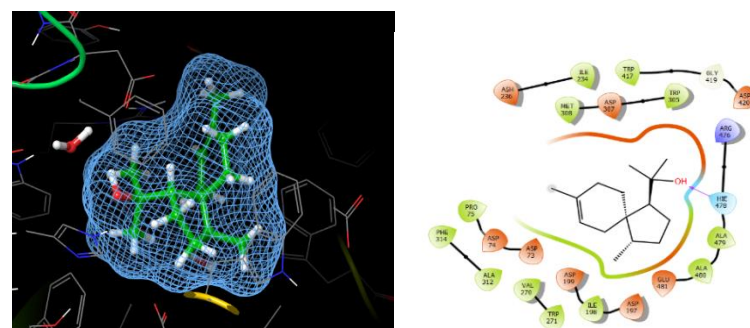
### Binding surface and 2D interaction diagram of compounds using PDB ID: 6C9X



**Figure 7: Xanthinin**



**Figure 8: Dibutyl phthalate**



**Figure 9: Aconerol**

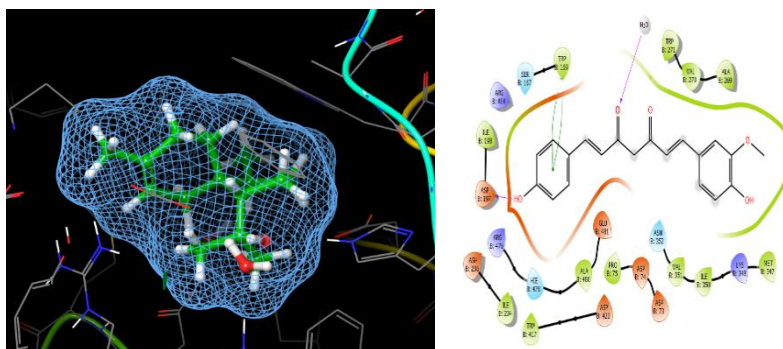


Figure 10: Desmethoxycurcumin

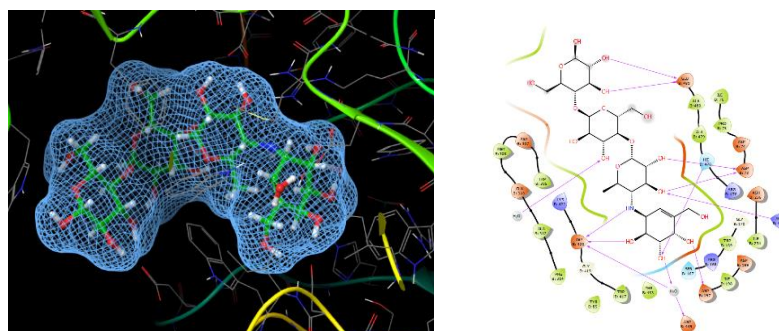


Figure 11: Acarbose

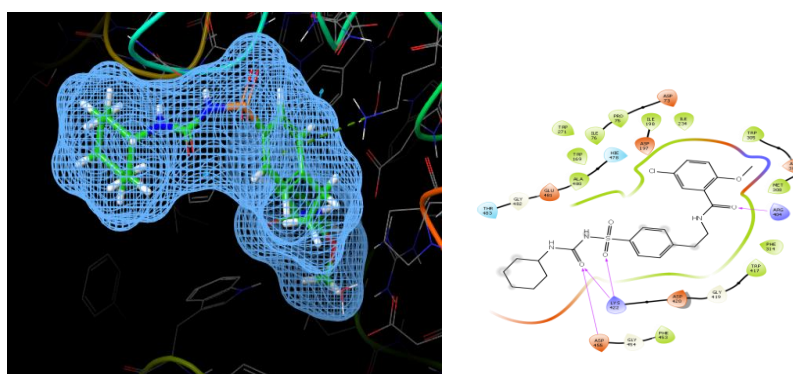


Figure 12: Glibenclamide

**Table 5:** Docking score of the most active compounds using PDB ID: 1ITU, and standard drug Acarbose, Glibenclamide

Compounds Name	Docking Score	Glide Emodel	Glide Energy	Residues of interaction
Dibutyl phthalate	-5.391	-37.839	-25.779	Asp288, Arg230, Zn402, Hie152, Tyr252, Val292, Pro293, Arg294
Arglabin	-5.305	-39.682	-27.996	Hie152, Val292, Pro293, Tyr252, Asn250, Gly291, Gln26, Asp22
Ivalin	-5.087	-40.858	-31.292	Tyr68, Hie152, Asp29, Cys71, Val292, Ser153, His20
Terpinen-4-ol	-4.933	-25.684	-19.274	Asp288, Gly291, His20, Thr9, Tyr68, His198, Gln26, Cys71
Acarbose	-4.697	-57.210	-45.799	Hie152, Cys71, Asp72, Asp288, Tyr68, Thr69, Ser153, Asp290
Glibenclamide	-6.535	-77.075	-51.184	Arg230, Hie152, Gly291, Tyr252

Molecular docking was used to examine the means by which the components of *C. caesia* bind to the associated receptors. A molecular docking study of *C. caesia* compounds and a common drug was carried out using the active site of dipeptidase (PDB ID: 1ITU) (acarbose). From a 2-D ligand

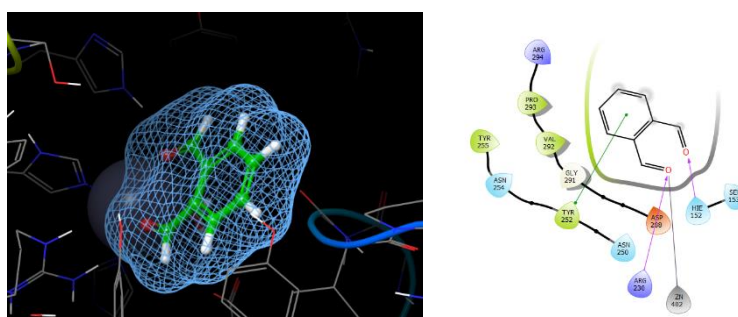
interaction diagrammatic standpoint, the oxygen atom of compounds' Ivalin amide nucleus formed hydrogen connections with Hie152 and Tyr68 amino acid residues. The Gly291 and Asp288 amino acid residues made hydrogen bonds with the Terpinen-4-ol amide compound's oxygen



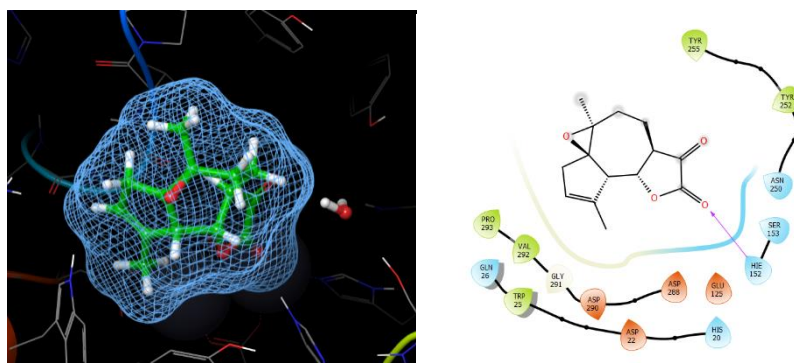
atom. The amino acid residues Hie152, Arg230, and Zn402 formed hydrogen bonds with the Dibutyl phthalate amide nucleus of the molecule. Hie152 amino acid residues formed hydrogen bonds with the amide nucleus of compound arglabin's oxygen atoms. The amino acid residues Cys71, Asp72, Hie152, Tyr68, and Asp288 formed hydrogen bonds with the oxygen atoms of the amide nucleus of the common medication acarbose. The docking scores, glide energy, and glide emodel numbers were displayed negatively. The ligand's affinity for binding to the receptor increases with decreasing docking score. The top

four compounds (Ivalin, Dibutyl phthalate, Terpinen-4-ol, and Argabin) as well as the reference drug are shown in Table 5 along with their docking data. Figures 13, 14, 15, 16, 17 and 18 show the docked molecules Ivalin, Dibutyl phthalate, Terpinen-4-ol, Argabin, and acarbose's binding surface and ligand interaction diagram, respectively. According to the diagrammatic viewpoint of 2-D ligand interaction, these compounds interact with homologous residues of amino acid to have the same homology as regular Acarbose.

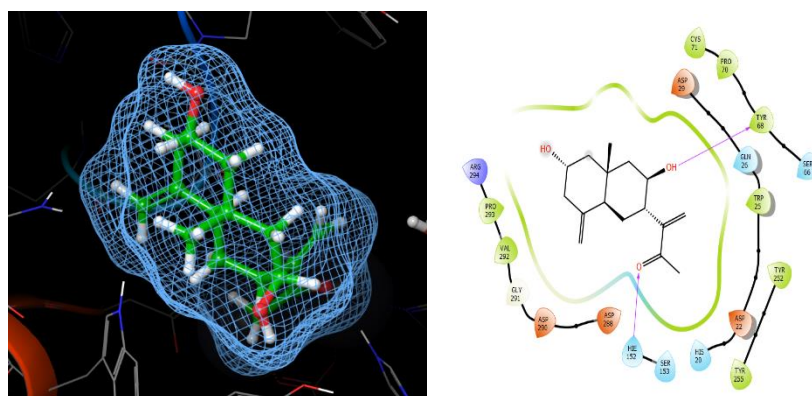
### Binding surface and 2D interaction diagram of compounds using PDB ID: 1ITU



**Figure 13: Dibutyl phthalate**



**Figure 14: Arglabin**



### Figure 15: Ivalin

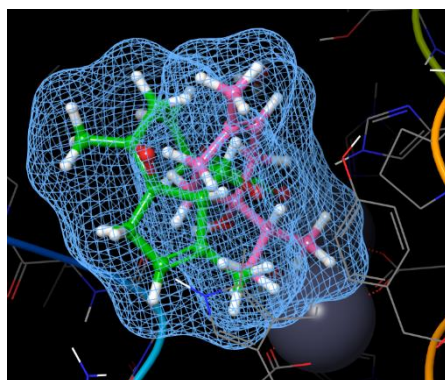


Figure 16: Terpinen-4-ol

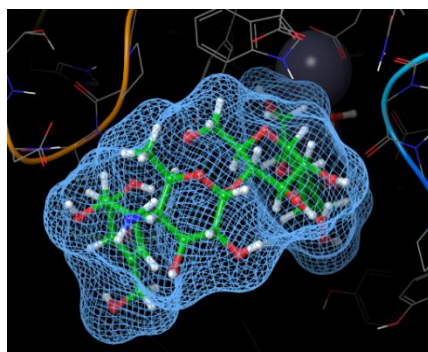


Figure 17: Acarbose

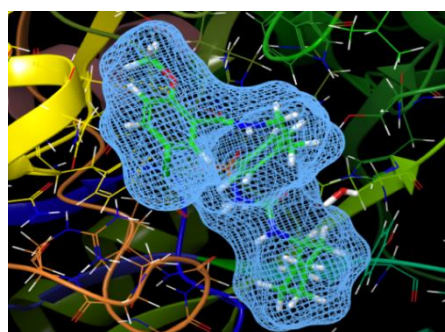


Figure 18: Glibenclamide

### ADME Study

Using the QikProp module for Schrodinger v 13.1, the ADME properties of the compounds of *C. caesia* given were identified. Aconerol, Argabin, Bisdemethoxycurcumin, Coniferol, Curcumin, Desmethoxycurcumin, Dibutyl phthalate, Ivalin, Terpinen-4-ol, and Xanthinin are some of the best active complexes whose ADME data are summarised in Table 6. The compounds Aconerol, Argabin, Bisdemethoxycurcumin, Coniferol,

Curcumin, Desmethoxycurcumin, Dibutyl phthalate, Ivalin, Terpinen-4-ol, and Xanthinin all adhered to the Lipinski rule of five. According to the conclusions, the compounds Aconerol, Argabin, Bisdemethoxycurcumin, Coniferol, Curcumin, Desmethoxycurcumin, Dibutyl phthalate, Ivalin, Terpinen-4-ol, and Xanthinin adhere to rule of Lipinski, suggesting that the compounds can be employed as model molecules for further investigation.

**Table 6:** ADME scoring of the most active constituents of *C. caesia*

Compounds Name	MW	donorHB	accptHB	QPlogPo/w	QPlogBB	Oral absorption in humans	Rule of Five
Aconerol	222.3	1	0.7	4.0	0.2	3	0
Argabin	248.2	1	5.7	1.1	-0.2	3	0
Bisdemethoxycurcumin	308.3	2	3.2	3.4	-2.0	3	0
Coniferol	180.2	2	3.2	1.3	-0.6	3	0
Curcumin	368.3	2	4.7	3.7	-2.1	3	0
Desmethoxycurcu	338.3	2	4.0	3.5	-2.1	3	0



min							
Dibutyl phthalate	134.1	0	4.0	0.2	-0.5	3	0
Ivalin	264.3	2	5.4	1.8	-0.7	3	0
Terpinen-4-ol	154.2	1	0.7	2.9	0.2	3	0
Xanthinin	152.1	3	5.0	-1.8	-1.0	2	0

- ✓ Molecular weight: 500 Da or less.
- ✓ Donor of hydrogen bonds (Accepted Maximum: 5)
- ✓ Acceptor of hydrogen bonds (Accepted Limit: 10)
- ✓ Log P low than 5.
- ✓ Human oral absorption is rated as low, medium, or high using 1, 2, or 3.
- ✓ QPlogBB values vary from -3.0 to 1.2.

## CONCLUSION

This study used a variety of computational methods, including molecular docking, ADME investigations, and compounds of *C. caesia* against alpha-glucosidase, alpha-amylase, and dipeptidase receptor. Coniferol, Bisdemethoxycurcumin, Desmethoxycurcumin, and curcumin have the highest docking scores against protein alpha-amylase according to molecular docking studies (PDB ID: 4GQR). With respect to protein alpha-glucosidase, compounds Xanthinin, Dibutyl phthalate, Desmethoxycurcumin, and Aconerol have the highest docking scores (PDB ID: 6C9X). Against protein dipeptidase, compounds Ivalin, Dibutyl phthalate, Terpinen-4-ol, and Argabin had the best docking scores (PDB ID: 1ITU). The compounds Aconerol, Argabin, Bisdemethoxycurcumin, Coniferol, Curcumin, Desmethoxycurcumin, Dibutyl phthalate, Ivalin, Terpinen-4-ol, and Xanthinin all exhibit an excellent ADME profile depends upon the results of molecular docking and binding interaction research. These substances (Aconerol, Argabin, Bisdemethoxycurcumin, Coniferol, Curcumin, Desmethoxycurcumin, Dibutyl phthalate, Ivalin, Terpinen-4-ol, and Xanthinin), according to the study, could be used as lead structures for further studies on anti-diabetic resistance.

## CONSENT FOR PUBLICATION

Not applicable

## CONFLICT OF INTEREST

The authors declare no conflict of interest.

## ACKNOWLEDGEMENTS

Declared none.

## REFERENCES

1. da Silva JA, de Souza ECF, Boschemeier AGE, et al, 2018. Diagnosis of diabetes mellitus and living with a chronic condition:

participatory study. BMC Public Health. 18, 1-8.

2. American Diabetes Association. 2009. Diagnosis and classification of diabetes mellitus. Diabetes Care. 32, S62-S67.
3. World Health Organization. 1999. Definition, diagnosis and classification of diabetes mellitus and its complications, Switzerland, Geneva.
4. Wild S, Roglic G, Green A, et al, 2004. Global prevalence of diabetes: estimates for the year 2000 and projections for 2030. Diabetes Care. 27(5), 1047-1053.
5. IDF. 2019. International Diabetes Federation Atlas, IDF, Aarhus, Denmark.
6. Bedekar, Shah K, Koffas M, et al, 2010. Natural products for type II diabetes treatment. Advances in Applied Microbiology, Elsevier, Amsterdam, Netherlands, 21-73.
7. Cerf ME. 2013. Beta cell dysfunction and insulin resistance. Frontier Endocrinology. 4,37.
8. Alam F, Shafique Z, Amjad ST, et al, 2019. Enzymes inhibitors from natural sources with antidiabetic activity: a review. Phytotherapy Research. 33(1), 41-54.
9. Chehade JM, Mooradian AD. 2000. A rational approach to drug therapy of type 2 diabetes mellitus. Drugs. 60(1), 95-113.
10. Kitada M, Zhang Z, Mima A, et al, 2010. Molecular mechanisms of diabetic vascular complications. Journal of Diabetes Investigation. 1(3), 77-89.
11. Mawahib C, Nabila Z, Nabila S, et al, 2019. LC-MS analysis, antioxidant and alpha-glucosidase inhibitory activities of Centaurea papposa extracts. Bangladesh Journal of Pharmacology. 14(4), 159-165.
12. Mukherjee PK, Kumar V, Mal M, et al, 2007. Acetylcholinesterase inhibitors from plants. Phytomedicine. 14(4), 289-300.
13. Notkins AL. 2002. Immunologic and genetic factors in type 1 diabetes. Journal of Biological Chemistry. 277(46), 43545-43548.
14. Ahamad Jand, Naquvi KJ. 2011. Review on role of natural alpha-glucosidase inhibitors for management of diabetes mellitus. International Journal of BioMed Research. 2(6), 374-380.
15. Chiasson JL, Josse RG, Gomis R, et al, 2002. Acarbose for prevention of type 2 diabetes mellitus: the STOP-NIDDM randomised trial. Ae Lancet. 359(9323), 2072-2077.

16. Lasano NF, Ramli NS, Hamid AH, et al, 2019. Effects of different extraction solvents on polyphenols and antioxidant capacity of peel, pulp and seed kernel of kuini (*Mangifera odorata*). *Oriental Pharmacy and Experimental Medicine*. 19(3), 277-286.
17. Acet T. 2020. Determining the phenolic components by using HPLC and biological activity of *Centaurea triumfetti*. *Plant Biosystems*. 155(1), 15.
18. Xu J, Cao J, Yue J, et al, 2018. New triterpenoids from acorns of *Quercus liaotungensis* and their inhibitory activity against  $\alpha$ -glucosidase,  $\alpha$ -amylase and protein-tyrosine phosphatase 1B. *Journal of Functional Foods*. 41, 232-239.
19. Dehghan H, Salehi P, Amiri MS, et al, 2018. Bioassay-guided purification of  $\alpha$ -amylase,  $\alpha$ -glucosidase inhibitors and DPPH radical scavengers from roots of *Rheum turkestanicum*. *Industrial Crops and Products*. 117, 303-309.
20. Karim Z, Holmes M, Orfila C et al, 2017. Inhibitory effect of chlorogenic acid on digestion of potato starch. *Food Chemistry*. 217, 498-504.
21. Tan Y, Chang SKC, Zhang Y, et al, 2017. Comparison of  $\alpha$ -amylase,  $\alpha$ -glucosidase and lipase inhibitory activity of the phenolic substances in two black legumes of different genera. *Food Chemistry*. 214, 259-268.
22. Dona AC, Pages G, Gilbert RG, et al, 2010. Digestion of starch: *In vivo* and *in vitro* kinetic models used to characterise oligosaccharide or glucose release. *Carbohydrate Polymers*. 80(3), 599-617.
23. Zheng Y, Yang W, Sun W, et al, 2020. Inhibition of porcine pancreatic  $\alpha$ -amylase activity by chlorogenic acid. *Journal of Functional Foods*. 64, 103587. <https://doi.org/10.1016/j.jff.2019.103587>
24. Tian JL, Si X, Wang YH, et al, 2021. Bioactive flavonoids from *Rubus corchorifolius* inhibit  $\alpha$ -glucosidase and  $\alpha$ -amylase to improve postprandial hyperglycemia. *Food Chemistry*. 341.
25. Zheng Y, Tian J, Yang W, et al, 2020. Inhibition mechanism of ferulic acid against  $\alpha$ -amylase and  $\alpha$ -glucosidase. *Food Chemistry*. 317, 126346. <https://doi.org/10.1016/j.foodchem.2020.126346>
26. Yogamaya D, Bandita D, Sahu RK, et al, 2012. Comparative antioxidant activity of non-enzymatic and enzymatic extracts of *Curcuma zedoaria*, *Curcuma angustifolia* and *Curcuma caesia*. *International Journal of Plant, Animal and Environmental Sciences*. 2, 232-239.
27. Borah A, Paw M, Gogoi R, et al, 2019. Chemical composition, antioxidant, anti-inflammatory, anti-microbial and in-vitro cytotoxic efficacy of essential oil of *Curcuma caesia* Roxb. leaves: An endangered medicinal plant of North East India. *Industrial Crops and Products*. 129, 448–454. doi:10.1016/j.indcrop.2018.12.035
28. Das S, Mondal P, Zaman MK, et al, 2013. *Curcuma caesia* Roxb. And its medicinal uses: a review. *International Journal of Research in Pharmacy and Chemistry*. 370-375.
29. Paliwal P, Pancholi SS, Patel RK, et al, 2011. Comparative evaluation of some plant extracts on bronchoconstriction in experimental animals. *Asian Journal of Pharmacy and Life Sciences*. 1, 52-57.
30. Sarangthem K, Haokip MJ. 2010. Bioactive components in *Curcuma caesia* Roxb. grown in Manipur. *Bioscan*. 5, 113-115.
31. Jose S, Thomas TD. 2014. Comparative phytochemical and anti-bacterial studies of two indigenous medicinal plants *Curcuma caesia* Roxb. and *Curcuma aeruginosa* Roxb. *International Journal of Green Pharmacy*. 8, 65-71.
32. Arulmozhi DK, Sridhar N, Veeranjanyulu A, et al, 2006. Preliminary mechanistic studies on the smooth muscle relaxant effect of hydroalcoholic extract of *Curcuma caesia*. *Journal of Herbal Pharmacotherapy*. 6(3/4), 117-124.
33. Jain A, Parihar DK. 2018. In vitro antioxidant and antidiabetic activity of regional chemotypes of three *Curcuma* species from Chhattisgarh. *Research and Reviews: Journal of Herbal Science*. 7, 13-22.
34. Karmakar I, Dolai N, Suresh Kumar RB, et al, 2013. Antitumor activity and antioxidant property of *Curcuma caesia* against Ehrlich's ascites carcinoma bearing mice. *Pharmaceutical Biology*. 51(6), 753-759.
35. Devi HP, Mazumder PB, Devi LP, et al, 2015. Antioxidant and antimutagenic activity of *Curcuma caesia* Roxb. rhizome extracts. *Toxicology Reports*. 2, 423-428.
36. Gupta VK, Kaushik A, Chauhan DS, et al, 2018. Anti-mycobacterial activity of some medicinal plants used traditionally by tribes from Madhya Pradesh, India for treating tuberculosis related symptoms. *Journal of Ethnopharmacology*. 227, 113-120.
37. Devi HP, Mazumder PB. 2016. Methanolic extract of *Curcuma caesia* Roxb. prevents the

- toxicity caused by cyclophosphamide to bone marrow cells, liver and kidney of mice. *Pharmacognosy Research*. 8, 43-49.
38. Hadanu R, Adelin L, Sutapa IW, et al, 2018. QSAR studies of nitrobenzothiazole derivatives as antimalarial agents. *Makara Journal of Science*. 22(1), 5.
39. Kapetanovic IM. 2018. Computer-aided drug discovery and development (CADD): in silico-chemico-biological approach. *Chem Biol Interact*. 171(2), 165-176.
40. Meng XY, Zhang HX, Mezei M, et al, 2011. Molecular Docking: A powerful approach for structure-based drug discovery. *Current Computer Aided Drug Design*. 7(2), 146-157.
41. Leelananda SP, Lindert S. 2016. Computational methods in drug discovery. *Beilstein Journal of Organic Chemistry*. 12, 2694-2718
42. Kumar S, Lim SM, Ramasamy K, et al, 2017. Synthesis, molecular docking and biological evaluation of bis-pyrimidine Schiff base derivatives. *Chemistry Central Journal*. 11(1), 1-6.
43. Sharma D, Kumar S, Narasimhan B, et al, 2019b. 4-(4-Bromophenyl)-thiazol-2-amine derivatives: synthesis, biological activity and molecular docking study with ADME profile. *BMC Chemistry*. 13, 1-6.
44. Chaturvedi M, Rani R, Sharma D, et al, 2019. Comparison of *Curcuma caesia* extracts for bioactive metabolite composition, antioxidant and antimicrobial potential. *Natural Product Research*. 3131-3135.
45. Dizdaroglu Y, Albay C, Arslan T, et al, 2020. Design, synthesis and molecular modelling studies of some pyrazole derivatives as carbonic anhydrase inhibitors. *Journal of Enzyme Inhibition and Medicinal Chemistry*. 35(1), 289-297.
46. Ramchandran Balaji, Kesavan S, Rajkumar T, et al, 2016. Molecular modeling and docking of small molecule inhibitors against NEK2. *Bioinformation*. 12(2), 62-68.
47. Pattar SV, Adhoni SA, Kamanavalli CM, et al, 2020. In silico molecular docking studies and MM/GBSA analysis of coumarin carbonodithioate hybrid derivatives divulge the anticancer potential against breast cancer. *Journal of Basic and Applied Sciences*. 9, 36.
48. Sharma V, Sharma PC, Kumar V, 2016. In silico molecular docking analysis of natural pyridoacridines as anticancer agents. *Advances in Chemistry*. 1-9.
49. Kaushik AC, Kumar S, Wei DQ, et al, 2018. Structure based virtual screening studies to identify novel potential compounds for GPR142 and their relative dynamic analysis for study of type 2 diabetes. *Frontiers in Chemistry*. 6, 1-14.
50. Meraj K, Mahto MK, Christina NB, et al, 2012. Molecular modeling, docking and ADMET studies towards the development of novel Disopyramide analogs for potential inhibition of human voltage-gated sodium channel proteins. *Bioinformatics*. 8(23), 1139.